

Pump-to-signal RIN transfer in dual-order silicon Raman amplifiers

XIQING LIU*, XINZHU SANG, XIAOXIA LIU, BINBIN YAN, KUIRU WANG, CHONGXIU YU
Key Laboratory of Information Photonics and Optical Communications (Beijing University of Posts and Telecommunications), Ministry of Education, Post Box 163(BUPT), Beijing 100876, China

Dual-order silicon Raman Amplifiers are analyzed and numerically discussed. The effect of relative intensity noise (RIN) transferred from second-order pump to signal in 1-cm long chip scale silicon Raman amplifiers is investigated. Similar to single-order silicon Raman Amplifiers, -3dB corner frequency of RIN transfer function in second-order silicon Raman Amplifiers is almost the same as that in single-order silicon Raman Amplifiers due to lack of sufficient “walk off” in short waveguide length. The noise figure of dual-order silicon Raman amplifiers is deteriorated than single-order silicon Raman Amplifiers.

(Received June 06, 2010; accepted July 14, 2010)

Keywords: Dual-order silicon Raman amplifiers, Noise figure, Silicon-on-insulator technology, Raman scattering

1. Introduction

Miniaturization of nonlinear optical devices in silicon waveguides has attracted considerable attention in recent years. Silicon-on-insulator (SOI) waveguides can realize monolithically integrated optical devices with electronic devices as a preferred platform. Nonlinear photonic phenomena and devices in silicon such as Raman amplification and lasing, optical modulation, wavelength conversion and parametric amplification, all-optical switching, and optical signal regeneration and so on, have been successfully demonstrated [1-7]. Raman amplification have been demonstrated for amplifying signal light. Single-order and dual-order Raman amplifiers are the basic approaches. Compared with the single-order configurations, dual-order Raman fiber amplifiers demonstrated improved noised figure, due to the more uniform distribution of the Raman gain [8]. RIN transfer is analyzed in both single-order and dual-order Raman fiber Amplifiers [9]-[10]. The low frequency second-order transfer function is about 15 dB higher than the low frequency first-order transfer function. The second-order pump generates gain fluctuations at the first-order pump wavelength and further impacts the fluctuations of the signal. Recently, we investigated RIN transfer in single-order silicon Raman amplifiers[11]. Due to small “walk off” in the short silicon waveguide, as high as 1.5GHz RIN frequency components are transferred to the signal, which deteriorates the final noise figure of the amplifier. In addition, cascaded silicon Raman lasers have been demonstrated and analyzed [12,13], where dual-order Raman gain should be used.

In this letter, we investigate the pump-to-signal RIN transfer and its contribution to the noise figure in

dual-order silicon Raman Amplification for the first time. We show that the net gain in second-order silicon Raman amplifiers is improved, and -3dB corner frequency of RIN transfer function is almost the same as that in single-order silicon Raman amplifiers, due to lack of sufficient “walk off” in short waveguide length. The noise figure is deteriorated than single-order silicon Raman amplifiers due to nonlinear losses including two-photon absorption (TPA) and free-carrier absorption (FCA).

2. Derivation of RIN transfer in dual-order silicon Raman amplifiers

In Dual-order silicon Raman amplifiers operating at 1550 nm, two pumps at $\lambda_{p1} = 1291\text{nm}$ and $\lambda_{p2} = 1418\text{nm}$ should be used. To evaluate the evolution and the noise of the optical intensity I_{p1} , I_{p2} , I_s , two important nonlinear losses of TPA and TPA-induced FCA are considered. Due to different group velocities at different wavelengths, the “walk off” between the pump and the signal is included in the following analyses. The interaction among the three waves on a reference plane traveling with the signal can given as,

$$\frac{\partial I_{p1}}{\partial z} - d_{1z} \frac{\partial I_{p1}}{\partial t} = -\alpha_{p1} I_{p1} - \alpha_{p1}^{FCA} I_{p1} - \beta_{TPA} I_{p1}^2 - 2 \cdot \beta_{TPA} (I_{p1} I_s + I_{p1} I_{p2}) - \frac{w_{p1}}{w_{p2}} g_{p1p2} I_{p1} I_{p2} - \frac{w_{p1}}{w_s} g_{p1s} I_{p1} I_s \quad (1)$$

$$\frac{\partial I_{p2}}{\partial z} - d_{2z} \frac{\partial I_{p2}}{\partial t} = -\alpha_{p2} I_{p2} - \alpha_{p2}^{FCA} I_{p2} - \beta_{TPA} I_{p2}^2 - 2 \cdot \beta_{TPA} (I_{p2} I_s + I_{p1} I_{p2}) + \frac{w_{p2}}{w_{p1}} g_{p1p2} I_{p1} I_{p2} - \frac{w_{p2}}{w_s} g_{p2s} I_{p2} I_s \quad (2)$$

$$\frac{\partial I_s}{\partial z} = \mp \alpha_s I_s \mp \alpha_s^{FCA} I_s \mp \beta_{TPA} I_s^2 \mp 2 \cdot \beta_{TPA} (I_{p1} + I_{p2}) I_s \pm g_{p1s} I_{p1} I_s \pm g_{p2s} I_{p2} I_s \quad (3)$$

The parameters I_{p1} , I_{p2} and I_s represent the intensities of the second-order pump, the first-order pump and the signal. $\alpha_{p1}, \alpha_{p2}, \alpha_s$ are the linear loss coefficients. g_{ij} ($i, j = p1, p2, s$) are the Raman gain coefficient and w_{p1}, w_{p2}, w_s are the angular frequencies. The signs "±" and "∓" represent the co propagating and counter propagating configurations, respectively. β_{TPA} is the two-photon absorption coefficient. The free-carrier absorption coefficient is

$$\alpha_j^{FCA}(z) = 1.45 \times 10^{-17} (\lambda_j / 1550)^2 N(z) \quad (j = p1, p2, s)$$

where $N(z)$ is the free-carrier density given

$$\text{by } N(z) = \frac{\tau \beta_{TPA}}{2h\nu} (I_{p1} + I_{p2} + I_s)^2. \quad \tau \text{ is the free-carrier}$$

lifetime. $h\nu$ is the photon energy. $N(z)$ is influenced by

the second-order pump, the first-order pump and the signal. The "walk off" parameters are given by $d_{1\pm} = \frac{1}{v_s} \mp \frac{1}{v_{p1}}$,

$d_{2\pm} = \frac{1}{v_s} \mp \frac{1}{v_{p2}}$, where v_{p1} , v_{p2} and v_s are the group

velocities in the silicon waveguide. For the copropagation

configuration, the "walk off" parameters d_{1+} and d_{2+} is mostly affected by the group velocity dispersion (GVD).

They are relevant to the local GVD and the wavelength separation $\Delta\lambda$. d_{1+} and d_{2+} can be described

$$\text{as } d_{1+} \approx D\Delta\lambda_1, \quad d_{2+} \approx D\Delta\lambda_2 \quad (\Delta\lambda_1 = \lambda_s - v_{p1}, \Delta\lambda_2 = \lambda_s - v_{p2}).$$

For the counter propagating configuration, the "walk off" parameter is primarily due to the opposing velocities, and

they are given by $d_{1-} \approx d_{2-} \approx 2n_g / c$ (n_g is the

average group index and c is the speed of light in vacuum). We can write the spatial and time-dependent optical intensity at any location along the silicon waveguide as follows:

$$I_{p1}(z, t) = \bar{I}_{p1}(z) [1 + N_1(z, t)] \quad (4)$$

$$\bar{I}_{p1}(z) [1 + n_1(z) \exp(i\omega t)]$$

$$I_{p2}(z, t) = \bar{I}_{p2}(z) [1 + N_2(z, t)] \quad (5)$$

$$\bar{I}_{p2}(z) [1 + n_2(z) \exp(i\omega t)]$$

$$I_s(z, t) = \bar{I}_s(z) [1 + M(z, t)] \quad (6)$$

$$\bar{I}_s(z) [1 + m(z) \exp(i\omega t)]$$

where $\bar{I}_{p1}(z)$, $\bar{I}_{p2}(z)$ and $\bar{I}_s(z)$ correspond to the steady-state optical intensities at location z and the bars represent a time average. The complex modulation indexes $N_1(z, t)$, $N_2(z, t)$, $M(z, t)$ can be separated by the complex spatial modulation indices $n_1(z)$, $n_2(z)$, $m(z)$ and sinusoidal time dependence $\exp(i\omega t)$ at an angular frequency ω . Substituting (4), (5), (6) into (1), (2) and (3), we can derive three differential equations for the steady-state optical intensity as follows and the complex spatial modulation indices:

$$\frac{\partial \bar{I}_{p1}}{\partial z} = -\alpha_{p1} \bar{I}_{p1} - \kappa_{p1} \cdot (\bar{I}_{p1} + \bar{I}_{p2} + \bar{I}_s)^2 \bar{I}_{p1} - \beta_{TPA} I_{p1}^2 - 2\beta_{TPA} \bar{I}_{p1} [\bar{I}_s + \bar{I}_{p2}] \quad (7)$$

$$- \frac{w_{p1}}{w_{p2}} g_{p1p2} \bar{I}_{p1} \bar{I}_{p2} - \frac{w_{p1}}{w_s} g_{p1s} \bar{I}_{p1} \bar{I}_s$$

$$\frac{\partial \bar{I}_{p2}}{\partial z} = -\alpha_{p2} \bar{I}_{p2} - \kappa_{p2} \cdot (\bar{I}_{p1} + \bar{I}_{p2} + \bar{I}_s)^2 \bar{I}_{p2} - \beta_{TPA} I_{p2}^2 - 2\beta_{TPA} \bar{I}_{p2} [\bar{I}_s + \bar{I}_{p1}] \quad (8)$$

$$+ \frac{w_{p2}}{w_{p1}} g_{p1p2} \bar{I}_{p1} \bar{I}_{p2} - \frac{w_{p2}}{w_s} g_{p2s} \bar{I}_{p2} \bar{I}_s$$

$$\frac{\partial \bar{I}_s}{\partial z} = \mp \alpha_s \bar{I}_s \mp \kappa_s \cdot (\bar{I}_{p1} + \bar{I}_{p2} + \bar{I}_s)^2 \bar{I}_s \mp \beta_{TPA} I_s^2 \mp 2\beta_{TPA} \bar{I}_s [\bar{I}_{p1} + \bar{I}_{p2}] \quad (9)$$

$$\pm g_{p1s} \bar{I}_s \bar{I}_{p1} \pm g_{p2s} \bar{I}_s \bar{I}_{p2}$$

$$\frac{\partial n_1}{\partial z} = i\omega n_1 \cdot d_{1\pm} - \beta_{TPA} \cdot \bar{I}_{p1} \cdot n_1 - 2\beta_{TPA} (\bar{I}_s \cdot m + \bar{I}_{p2} \cdot n_2) \quad (10)$$

$$- \frac{w_{p1}}{w_{p2}} g_{p1p2} \bar{I}_{p2} \cdot n_2 - \frac{w_{p1}}{w_s} g_{p1s} \bar{I}_s \cdot m - 2\kappa_{p1} \nabla$$

$$\frac{\partial n_2}{\partial z} = i\omega n_2 \cdot d_{2\pm} - \beta_{TPA} \cdot \bar{I}_{p2} \cdot n_2 - 2\beta_{TPA} (\bar{I}_s \cdot m + \bar{I}_{p1} \cdot n_1) \quad (11)$$

$$+ \frac{w_{p2}}{w_{p1}} g_{p1p2} \bar{I}_{p1} \cdot n_1 - \frac{w_{p2}}{w_s} g_{p2s} \bar{I}_s \cdot m - 2\kappa_{p2} \nabla$$

$$\frac{\partial m}{\partial z} = -\beta_{TPA} \bar{I}_s m - 2\beta_{TPA} (\bar{I}_{p1} \cdot n_1 + \bar{I}_{p2} \cdot n_2) + g_{p1s} \cdot \bar{I}_{p1} \cdot n_1 \quad (12)$$

$$+ g_{p2s} \cdot \bar{I}_{p2} \cdot n_2 - 2\kappa_s \nabla$$

where

$$\nabla = \bar{I}_{p1}^2 n_1 + \bar{I}_{p1} \bar{I}_{p2} n_2 + \bar{I}_{p1} \bar{I}_s m + \bar{I}_{p1} \bar{I}_{p2} n_1 + \bar{I}_{p2}^2 n_2$$

$$+ \bar{I}_{p2} \bar{I}_s m + \bar{I}_{p1} \bar{I}_s n_1 + \bar{I}_{p2} \bar{I}_s n_2 + \bar{I}_s^2 m$$

$$\text{and} \quad \kappa_j = \alpha_j^{FCA} / I^2 \quad (j = p1, p2, s)$$

Assuming that $|n_1|^2$, $|n_2|^2$, $|m|^2$, $|n_1 \cdot m|$, $|n_2 \cdot m|$, $|n_1 \cdot n_2| \ll 1$, quadratic modulation terms can be neglected. The RIN transfer for co propagating and counter propagating dual-order silicon Raman amplifiers can be calculated based on the following equations:

$$T_{3i}^+(L, \omega) = \frac{|M(L, \omega)|^2}{|N_i(0, \omega)|^2} \quad (13)$$

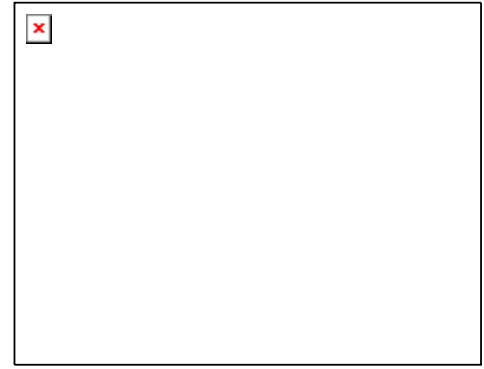
$$T_{3i}^-(0, \omega) = \frac{|M(0, \omega)|^2}{|N_i(0, \omega)|^2} \quad (14)$$

where $i = 1, 2$ corresponds to the RIN transfer generated by the first-order pump and the second-order pump, respectively. The above equations can be solved numerically, and we can obtain RIN transfer functions of dual-order silicon Raman amplifiers for co-propagating and counter-propagating configurations, respectively.

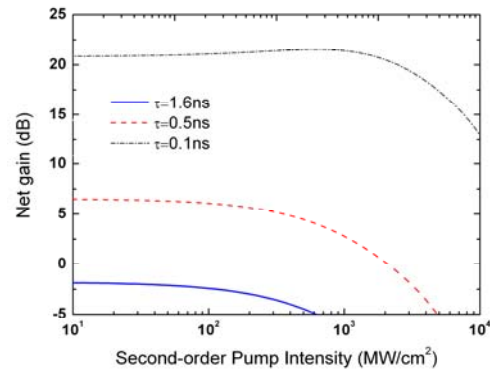
3. Results

3.1 Pump-to-signal RIN transfer in dual-order silicon Raman amplifiers

The waveguide parameters of RIN transfer calculated in dual-order silicon Raman amplifiers are used as follows: the waveguide length L is 1cm, the linear loss $\alpha_{p1} = \alpha_{p2} = \alpha_s = 1\text{dB/cm}$, 1291~1418nm Raman gain coefficient $g_{p1p2} = 18\text{cm/GW}$, 1291~1550nm Raman gain coefficient $g_{p1s} = 1.5\text{cm/GW}$, 1418~1550nm Raman gain coefficient $g_{p2s} = 15\text{cm/GW}$, TPA coefficient $\beta_{TPA} = 0.7\text{cm/GW}$. To evaluate the impact of “walk off”, the GVD parameter is $D = -910\text{ps}/(\text{nm} \cdot \text{km})$, the same as in [11]. The effective mode area is $1\mu\text{m}^2$. The signal intensity I_s is much smaller than the second-order pump intensity I_{p2} and first-order pump intensity I_{p1} . We also neglect the impact of pumps’ depletion due to Raman gain. Fig. 1 (a) and (b) show net Raman gain for first-order pump intensity at $I_{p2} = 200\text{MW/cm}^2$ and 1000MW/cm^2 respectively as dual-order pump intensity varying from 1 to 10^4MW/cm^2 . For $\tau = 0.1\text{ns}$, net gain reaches 16.8dB at $I_{p1} = 200\text{MW/cm}^2$, which is about 9dB greater than single-order amplifiers. With I_{p1} increasing, the net gain enters into saturation and decreases. As τ increases, the net gain will not be improved and even decreased especial for large I_{p1} . In Fig.1 (b), the net gain can only reach 21.97dB $I_{p1} = 1000\text{MW/cm}^2$ for $\tau = 0.1\text{ns}$, it only improves by 1.2dB by compared with single-order pump. Dual-order pump intensities I_{p1} and I_{p2} have an impact on free carriers, which will decrease the net gain with τ increasing.



(a)



(b)

Fig. 1. (a) Net Raman gain versus dual-order pump intensity with $I_{p2} = 200\text{MW/cm}^2$ (b) Net Raman gain versus dual-order pump intensity with $I_{p2} = 1000\text{MW/cm}^2$

Fig. 2 (a) and (b) show the magnitude of the pump to signal RIN transfer in single-order and dual-order silicon Raman amplifiers with free carrier lifetime $\tau = 0.1\text{ns}, 0.5\text{ns}, 1.6\text{ns}$ for co-pumped and counter-pumped configurations, respectively. The first-order pump intensity and the second-order pump intensity are equal, $I_{p2} = I_{p1} = 200\text{MW/cm}^2$. The pump intensities changed to 1000MW/cm^2 in Fig.(3). The RIN transfer function in single-order silicon Raman amplifiers agree with the results in [11]. From Fig.2 (a) and (b), we can see that the magnitude of RIN transfer in the dual-order silicon Raman amplifier is about 4dB higher than that in the single-order silicon Raman amplifier for $\tau = 0.1\text{ns}$. However it decrease about 1dB for $\tau = 1.6\text{ns}$. The RIN transfer depends on the Raman gain. The free carrier absorption FCA is influenced by I_{p1}, I_{p2}, τ . The -3dB corner frequency of dual-order silicon Raman amplifiers is about 400 GHz and 1.5 GHz for co and counter propagation, respectively. It is almost the same with single-order silicon Raman amplifiers. The main reason is that the “walk off” in 1cm length silicon waveguide is inefficient to average the pump intensity noise.

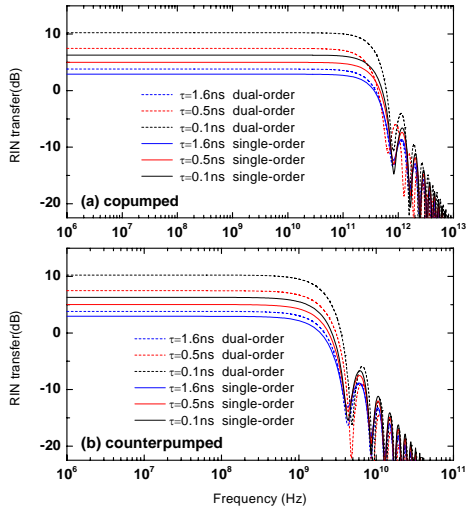


Fig. 2. RIN transfer spectra for co pumped (a) and counter pumped (b) in single-order (real line) and dual-order (dashed line) silicon Raman amplifiers.

$I_{p1} = I_{p2} = 200 \text{ MW/cm}^2$ Modal parameters: $L = 1 \text{ cm}$,
 $\lambda_{p1} = 1291 \text{ nm}$ $\lambda_{p2} = 1418 \text{ nm}$, $\lambda_s = 1550 \text{ nm}$,
 $\alpha_{p1} = \alpha_{p2} = \alpha_s = 1 \text{ dB/cm}$, $g_{p1p2} = 18 \text{ cm/GW}$,

$$g_{p1s} = 1.5 \text{ cm/GW}, g_{p2s} = 15 \text{ cm/GW}, \beta_{TPA} = 0.7 \text{ cm/GW}.$$

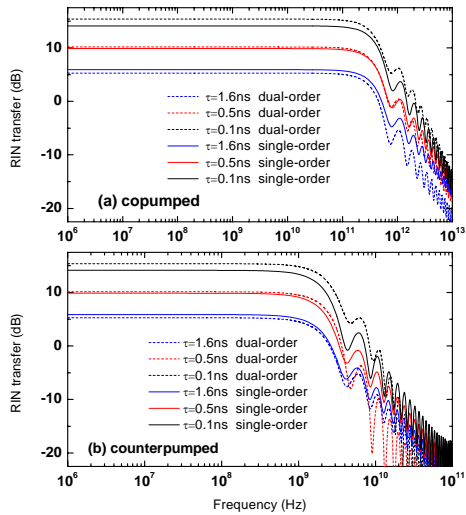
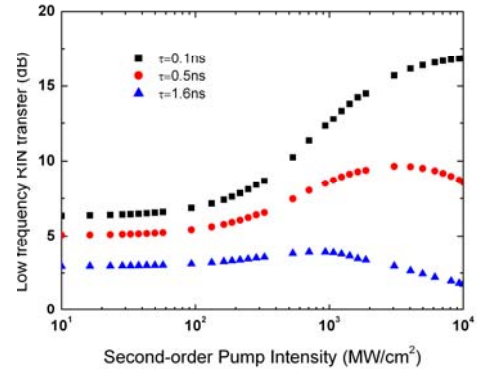


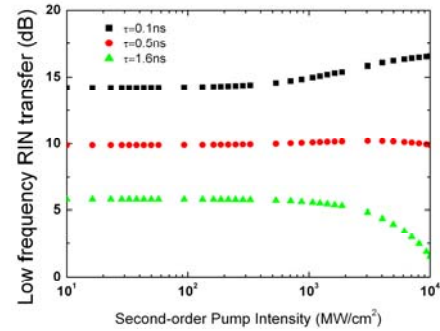
Fig. 3. RIN transfer spectra for co pumped (a) and counter pumped (b) in single-order (real line) and dual-order (dashed line) silicon Raman amplifiers.

$I_{p1} = I_{p2} = 1000 \text{ MW/cm}^2$ Modal parameters: $L = 1 \text{ cm}$, $\lambda_{p1} = 1291 \text{ nm}$,
 $\lambda_{p2} = 1418 \text{ nm}$, $\lambda_s = 1550 \text{ nm}$, $\alpha_{p1} = \alpha_{p2} = \alpha_s = 1 \text{ dB/cm}$,
 $g_{p1p2} = 18 \text{ cm/GW}$, $g_{p1s} = 1.5 \text{ cm/GW}$, $g_{p2s} = 15 \text{ cm/GW}$,
 $\beta_{TPA} = 0.7 \text{ cm/GW}$.

Fig. 4 (a) and (b) shows the low-frequency RIN transfer in dual-order silicon Raman amplifiers for first-order pump intensity $I_{p2} = 200 \text{ MW/cm}^2, 1000 \text{ MW/cm}^2$ respectively along with the second-order pump intensity I_{p1} varying from 10 to 10^4 MW/cm^2 . Due to the impact of Raman gain on RIN transfer, dual-order RIN transfer could be 9 dB higher than single-order RIN transfer at $\tau = 0.1 \text{ ns}$. It decreases to 1dB when $\tau = 1.6 \text{ ns}$. Whether there is net Raman gain or not, the pump noise will be transferred into the signal due to RIN transfer.



(a)



(b)

Fig. 4. (a) Low frequency RIN transfer versus dual-order pump intensity. $I_{p2} = 200 \text{ MW/cm}^2$; (b) Low frequency RIN transfer versus dual-order pump intensity. $I_{p2} = 1000 \text{ MW/cm}^2$.

3.2 Noise figure of dual-order silicon Raman amplifiers

Photo fluctuations along the gain medium can determine the noise figure of silicon Raman amplifier including nonlinear losses [6]. For high noise pump lasers with RIN of -125 dB/Hz the noise figure degrades by 11dB in the silicon Raman amplifiers with $\tau = 0.1 \text{ ns}$ [11]. Fig.5 (a) shows the noise figure of single-order (real line)

and second-order (dashed line) silicon Raman amplifiers under different τ with I_{p1} and I_{p2} varying from 10^{-1} to 10^3 MW/cm^2 . Fig.5 (b) gives the noise figure in dual-order silicon Raman amplifiers for different τ where $I_{p2} = 200 \text{ MW/cm}^2$ (real line), 1000 MW/cm^2 (dashed line), and I_{p1} vary from 10^{-1} to 10^3 MW/cm^2 . We can see that the noise figure degrades about 3.5dB with $I_{p1} = I_{p2} = 1000 \text{ MW/cm}^2$ and $\tau = 1.6 \text{ ns}$. It reduces to 1.4dB for $\tau = 0.1 \text{ ns}$. In Fig. 5 (b), the noise figure increase along with increasing pump intensity I_{p1} . The main reasons for noise figure deterioration in dual-order silicon Raman amplifiers lies in enhanced nonlinear losses and RIN transfer.

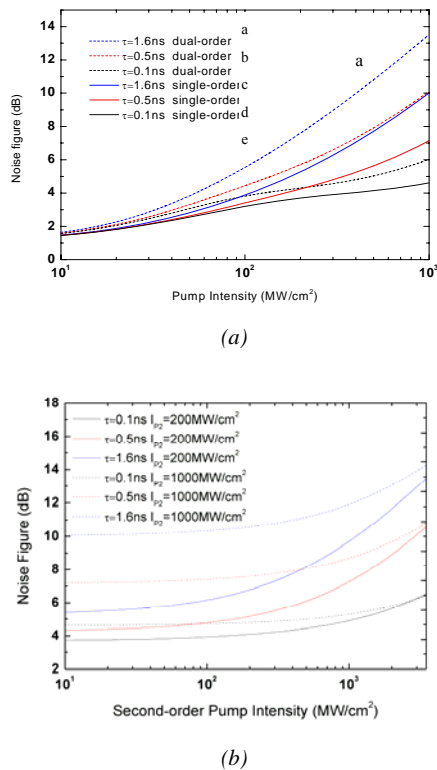


Fig. 5. (a) Noise figure of single-order (real line) and dual-order (dashed line) silicon Raman amplifiers with I_{p1} and I_{p2} varying from 10^{-1} to 10^3 MW/cm^2 ; (b) Noise figure of dual-order silicon Raman amplifiers with I_{p1} varying from 10^{-1} to 10^3 MW/cm^2 . $I_{p2} = 200 \text{ MW/cm}^2$ (real line), 1000 MW/cm^2 (dashed line).

4. Conclusions

RIN transferred from pump-to-signal in dual-order silicon Raman amplifiers have been investigated. We show that the RIN transfer in dual-order silicon Raman

amplifiers is related to second-order pump intensity I_{p1} and free carrier lifetime τ . Due to inefficient “walk off” in chip scale silicon Raman amplifiers, the “-3dB” corner frequency in dual-order amplifiers is consistent with single-order amplifier. The net gain can be improved with second-order pump for short free carrier lifetime. The noise figure of dual-order silicon Raman amplifiers is deteriorated due to enhancement in nonlinear losses. By properly choosing I_{p1} and τ , we can get high net gain, low RIN transfer and noise figure.

Acknowledgments

This work is partly supported by the National Key Basic Research Special Foundation (2010CB327601), the Key Project of Chinese Ministry of Education (No.109015), the National Science Foundation of China (60807022), and the Specialized Research Fund for the Doctoral Program of Higher Education (20070013001).

References

- [1] O. Boyraz, B. Jalali, *Electron. Express* **1**, 429 (2004).
- [2] H. Rong, R. Jones, A. Liu, O. Cohen, D. Hak, A. Fang, M. Paniccia, *Nature* **433**, 725 (2005).
- [3] X. Sang, E.-K. Tien, N. S. Yuksek, F. Qian, Q. Sang, O. Boyraz, *IEEE Photon. Technol. Lett.* **20**, 1184 (2008).
- [4] Y. -H. Kuo, H. Rong, V. Sih, S. Xu, M. Paniccia, O. Cohen, *Opt. Express* **14**, 11721 (2006)
- [5] X. Sang, E.-K. Tien, O. Boyraz, *J. Optoelectron. Adv. Mater.* **11**(1), 15 (2009).
- [6] X. Sang, O. Boyraz, *Opt. Express* **16**, 13122 (2008).
- [7] R. Salem, M. A. Foster, A. C. Turner et al, *Nature Photonics* **2**, 35 (2008).
- [8] J. Bouteiller, K. Brar, S. Radic, J. Bromage, Z. Wang, C. Headley, in *Proc. Optical Fiber Communications Conf. 2002*, Postdeadline paper FB3.
- [9] C. R. S. Fludger, V. Handerek, R. J. Mears, *J. Lightw. Technol.* **19**, 1140 (2001).
- [10] M. D. Mermelstein, K. Brar, C. Headley, *J. Lightw. Technol.* **21**, 1518 (2003).
- [11] X. Sang, D. Dimitropoulos, B. Jalali, O. Boyraz, *IEEE Photon. Technol Lett.* **20**, 1041 (2008)
- [12] H. Rong, S. Xu, O. Chohen, O. Raday, M. Lee, V. Sih, M. Paniccia, *Nature Photonics* **2**, 170 (2008).
- [13] M. Krause, R. Draheim, H. Renner, E. Brinkmeyer, *Electron Lett.* **42**, 1224 (2006).

*Corresponding author: xsang@bupt.edu.cn